Acta Chemica Scandinavica, 1999: 53: 1054–1058
Printed in UK. All rights reserved

ACTA
CHEMICA SCANDINAVICA
ISSN 0904-213X

Experimental and Theoretical Investigation of the UV Spectrum and Kinetics of the Aminomethyl Radical, $^{\cdot}CH_2NH_2$

Thomas la Cour Jansen,[a,*] Ib Trabjerg,[a] Sten Rettrup,[a] Palle Pagsberg[b] and Alfred Sillesen[b]

[a]Department of Chemistry, University of Copenhagen, Universitetsparken 5, DK-2100 Copenhagen Ø, Denmark and [b]Chemical Reactivity Section, Plant Biology and Biogeochemistry Department, Risø National Laboratory, DK 4000 Roskilde, Denmark

Jansen, T. l. C., Trabjerg, I., Rettrup, S., Pagsberg, P. and Sillesen, A., 1999. Experimental and Theoretical Investigation of the UV Spectrum and Kinetics of the Aminomethyl Radical, $^{\cdot}CH_2NH_2$. – Acta Chem. Scand. 53: 1054–1058. © Acta Chemica Scandinavica 1999.

The aminomethyl radical was produced by the reaction $F^{\cdot} + CH_3NH_2 \rightarrow HF + {}^{\cdot}CH_2NH_2$, which was initiated by pulse radiolysis of CH_3NH_2–SF_6 mixtures. The ultraviolet absorption spectrum of CH_2NH_2 was recorded on a timescale of 2 μs using a gated optical multichannel analyzer. The vibronic structure observed in the range 270–380 nm was analyzed by comparison with the results of *ab initio* calculations. Kinetics of the self-reaction $2\,{}^{\cdot}CH_2NH_2 \rightarrow$ products was studied by monitoring the transient absorption of $^{\cdot}CH_2NH_2$ at 319.5 nm. A value of $k = 8.1 \times 10^{-11}$ cm^3 molecule^{-1} s^{-1} was derived from the observed second-order kinetics combined with an estimated yield of the radical. In the presence of oxygen the decay rate was found to increase in accordance with the reaction $^{\cdot}CH_2NH_2 + O_2 \rightarrow$ products proceeding with a rate constant of $7.8(8) \times 10^{-11}$ cm^3 molecule^{-1} s^{-1}.

Oxidation of methylamine in the atmosphere is initiated by reaction with hydroxyl radicals, and has been studied previously by monitoring the decay rate of $^{\cdot}OH$.[1]

$$^{\cdot}OH + CH_3NH_2 \rightarrow H_2O + {}^{\cdot}CH_2NH_2 \quad (1a)$$

$$^{\cdot}OH + CH_3NH_2 \rightarrow H_2O + CH_3NH \quad (1b)$$

Because of the difference in bond energies,

$D(H\text{–}CH_2NH_2) = 94.6(2.0)$ kcal mol^{-1}

and

$D(CH_3NH\text{–}H) = 103(2)$ kcal mol^{-1}

it is proposed that reaction (1a) predominates. Based on an overall rate constant of $k_1 = 2.2 \times 10^{-11}$ cm^3 molecule^{-1} s^{-1} at 299 K the tropospheric lifetime of CH_3NH_2 was estimated to be about 3 h. The following reactions of CH_2NH_2 with O_2 and NO have been proposed.[2]

$$^{\cdot}CH_2NH_2 + O_2 \rightarrow {}^{\cdot}OOCH_2NH_2 \quad (2)$$

$$^{\cdot}OOCH_2NH_2 + NO \rightarrow {}^{\cdot}OCH_2NH_2 + NO_2 \quad (3)$$

$$^{\cdot}OCH_2NH_2 \rightarrow HCHO + {}^{\cdot}NH_2 \quad (4)$$

$$^{\cdot}OCH_2NH_2 + O_2 \rightarrow OCHNH_2 + HO_2^{\cdot} \quad (5)$$

* To whom correspondence should be addressed.

The radical $^{\cdot}CH_2NH_2$ produced by pulsed laser photolysis of ethylenediamine has been observed by photoionization mass spectrometry and a value of $k_2 = 3.5 \times 10^{-11}$ cm^3 molecule^{-1} s^{-1} has been reported.[3] In the present investigation we have recorded the ultraviolet spectrum of $^{\cdot}CH_2NH_2$ produced in the reaction of F-atoms with methylamine. The spectral features have been analyzed by *ab initio* calculations.

Experimental

The experimental set-up for pulse radiolysis combined with time-resolved ultraviolet spectroscopy has previously been described in detail.[4] High yields of F-atoms were obtained by radiolysis of SF_6, which was used as bath gas with a total pressure of 1 atm. In the presence of a small mole fraction of methylamine all F-atoms reacted by abstraction of H-atoms producing radicals of which only $^{\cdot}CH_2NH_2$ was identified. The ultraviolet spectrum of $^{\cdot}CH_2NH_2$ was recorded with an optical multichannel analyzer on a timescale of a few microseconds. Kinetic studies were carried out by monitoring the transient absorption of $^{\cdot}CH_2NH_2$ at 319.5 nm.

UV spectrum of $^{\cdot}CH_2NH_2$. Reactions (6a) and (6b) were initiated by pulse radiolysis of SF_6 containing a small mole fraction of methylamine.

$$F^{\cdot} + CH_3NH_2 \rightarrow HF + {}^{\cdot}CH_2NH_2 \quad (6a)$$

$$F^{\cdot} + CH_3NH_2 \rightarrow HF + {}^{\cdot}CH_3NH \quad (6b)$$

Figure 1 shows the ultraviolet spectrum of a short-lived radical which has been assigned the structure $^{\cdot}CH_2NH_2$. The spectrum was recorded with an optical multichannel analyzer on a timescale of 2 μs. The electronic transitions of $^{\cdot}CH_2NH_2$ appear to be similar to the Rydberg transitions of the isoelectronic radical $^{\cdot}CH_2OH$.[5,6] Based on the relative intensities and the bandshapes of the vibronic progression it seems obvious that at least two different electronic transitions are involved. The low energy transition 'a' with the 0–0 band situated at 368.6 nm is composed of a fairly strong vibronic progression with an average spacing of $\Delta\nu = 830\ cm^{-1}$. The strong and sharp 0–0 band 'b' at 319.5 nm was identified as the origin of a stronger electronic transition involving a complex mixture of vibronic progressions coupled with sharp antiresonances. A detailed analysis of the spectral features is presented in the theoretical section.

Kintics of $^{\cdot}CH_2NH_2$. The kinetics of $^{\cdot}CH_2NH_2$ were studied by monitoring the transient absorption at 319.52 nm. Figure 2 shows the kinetics of the self-reaction of $^{\cdot}CH_2NH_2$, which is most likely a combination reaction (7a) although the disproportionation reaction (7b) cannot be ruled out.

$$^{\cdot}CH_2NH_2 + {}^{\cdot}CH_2NH_2 \rightarrow H_2N\text{–}CH_2CH_2\text{–}NH_2 \quad (7a)$$

$$^{\cdot}CH_2NH_2 + {}^{\cdot}CH_2NH_2 \rightarrow CH_3NH_2 + CH_2NH \quad (7b)$$

Based on reported values of $\Delta H_{f,298}$/kcal mol^{-1} for $^{\cdot}CH_2NH_2$ (33.5),[7,8] CH_3NH_2 (−5.5)[9] and CH_2NH

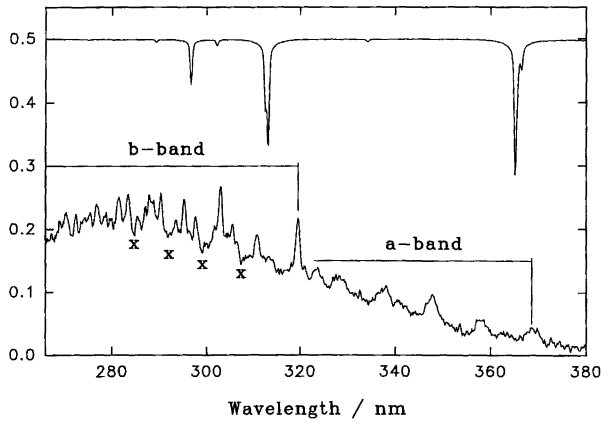

Fig. 1. UV spectrum of CH_2NH_2 produced by pulse radiolysis of a gas mixture containing 1 mbar CH_3NH_2 backed up with SF_6 to a total pressure of 1 atm. Wavelength calibration was carried out using the positions of the mercury lines shown on top. Band heads of two Rydberg transitions have been identified, a ($\pi^* \rightarrow 3p_x$) and b ($\pi^* \rightarrow 3p_y$). Sharp antiresonances are marked by ×.

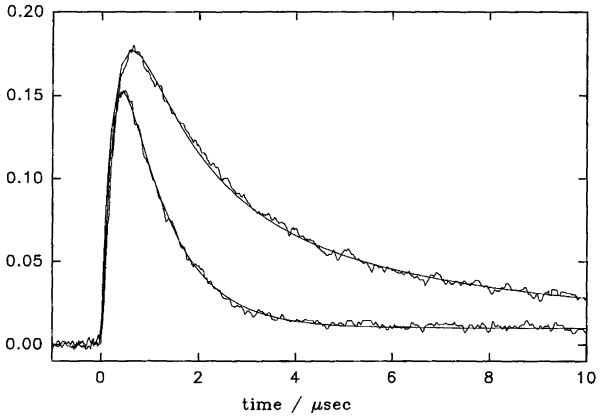

Fig. 2. Upper curve: kinetics of the reactions (7a) and (7b) monitored at 319.5 nm. Lower curve: pseudo-first-order kinetics observed in the presence of 1 mbar O_2.

(22),[10] reaction (7b) should be exothermic by about 50 kcal mol^{-1}. The kinetic features were analyzed by computer modeling using the CHEMSIMUL program.[11] By use of a simple model including only the reactions (6a) and (7a) the experimental curve shown in Fig. 2 could be fitted within the signal-to-noise ratio after adjustment of the rate constants, $k_{6a} = 1.3 \times 10^{-10}$ cm^3 molecule^{-1} s^{-1} and $k_{7a} = 8.1 \times 10^{-11}$ cm^3 molecule^{-1} s^{-1}. The value of k_{6a} may be taken with confidence while the value of k_{7a} represents a lower limit based on the assumption that all F-atoms are consumed in reaction (6a).

In the presence of oxygen the decay rate of CH_2NH_2 was found to increase with increasing oxygen concentrations, as shown in Fig. 2b. The addition reaction (8a) was proposed by Atkinson[2] while the formation of methyleneimine via (8b) has been discussed by Schade and Crutzen.[3]

$$^{\cdot}CH_2NH_2 + O_2 + M \rightarrow {}^{\cdot}OOCH_2NH_2 + M \quad (8a)$$

$$^{\cdot}CH_2NH_2 + O_2 \rightarrow CH_2NH + HO_2^{\cdot} \quad (8b)$$

The decay rate of the radical was studied as a function of oxygen concentration in the range $p(O_2) =$ 0.5–1.5 mbar, and, based on computer simulations of the experimental curves, we have determined a value of $k_8 = k_{8a} + k_{8b} = 7.8 \times 10^{-11}$ cm^3 molecule^{-1} s^{-1} at a total pressure of 1 atm. This value may be compared with the value of $k_8 = 3.5 \times 10^{-11}$ cm^3 molecule^{-1} s^{-1} determined by Washida *et al.* at total pressures in the range 0.6–6 Torr,[12] where the overall rate constant was found to remain constant. However, the difference between the rate constants obtained at different pressures may be taken as evidence for the occurrence of the pressure-dependent reaction (8a). Schade and Crutzen[13] have proposed that reaction (8b) may be a major channel in the atmospheric oxidation mechanism of methylamine. In the case of methanol we observed the analogous reaction $^{\cdot}CH_2OH + O_2 \rightarrow CH_2O + HO_2^{\cdot}$.[14] Thus, it appears that both reactions (8a) and (8b) contribute to the atmospheric oxidation of methylamine. Oxidation of

the intermediate product methyleneimine may give rise to the formation of HCN and N_2O,[13] which we intend to study by another experimental technique based on pulse radiolysis combined with infrared diode laser spectroscopy.[15] Formation and decay of the intermediate CH_2NH may be studied by scanning characteristic regions of the IR spectrum.[16]

Theoretical

Properties of $^{\cdot}CH_2NH_2$ in the ground state. Ab initio calculations were carried out using a basis set consisting of primitive Gaussian functions (C,N/13,8,3) and (H/4) contracted as ⟨C,N/7,6,3⟩ and ⟨H,2⟩ with spherical components of the d functions included in the calculation. These functions are the s, p and d functions from the VTZ basis set from the MOLPRO basis set library[17] for C and N and the s functions from the DZ basis set by Dunning for H.[18] The basis set was augmented with 3 primitive s, 3 primitive p and 1 primitive d functions on the heavy atoms; these are diffuse to ensure a good description of the Rydberg states (Table 1). In total the basis set consisted of 88 contracted functions. The geometry of $^{\cdot}CH_2HN_2$ has been calculated with the Restricted Open-shell Hartree–Fock (ROHF) method.[19] The ground state geometry, with C_s symmetry presented in Cartesian coordinates in Table 2, is similar to the geometry found previously by Dyke *et al.*[20] The vertical ionization potential was estimated to be 6.6 eV based on the ΔSCF method. The excitation energies were calculated with the same basis set and the geometry derived by the ROHF method using Multi Reference Configuration Interaction (MCRI)[21,22] with reference functions from an intermediate Complete Active Space Self Consistent Field (CASSSF) calculation[23–25] with the six states of lowest energy as reference states: four with A' symmetry and two with A'' symmetry. The complete active space had three electrons in six active orbitals resulting in 55 determinants of A' symmetry and 35 of A'' symmetry. The six states were optimized with equal weight and identified using symmetry and energy considerations. The MRCI calculation optimized the same six states with equal weight using single and double excitation in the entire space resulting in 417 206 configurations for calculations on A' symmetry states and 412 454 for A'' symmetry states. The calculations were done using the program package MOLPRO.[17] The vibrational frequencies for the ground state have been calculated using the TVZP basis set used by Dyke *et al.*[20] This calculation was performed with CADPAC[26] and the values here calculated at the SCF level are shown in Table 3. The vibrational frequencies calculated in this way are usually expected to be approximately 10% too high.

Table 1. Exponents for diffuse functions in the basis set.

Carbon		Nitrogen	
Function	Exponent	Function	Exponent
s	0.044020	s	0.057600
s	0.015080	s	0.018566
s	0.005166	s	0.005984
p	0.035690	p	0.049100
p	0.010536	p	0.013976
p	0.003110	p	0.003978
d	0.100000	d	0.151000

Table 2. The geometry of CH_2NH_2 in Cartesian coordinates (atomic units).

Atom	*x*	*y*	*z*
C	0.000000000	0.000000000	0.000000000
N	2.583093906	0.000000000	0.000000000
H1	−0.927206002	0.502291695	−1.753583606
H2	−0.927206002	0.502291695	1.753583606
H3	3.428970380	−0.639031080	1.568788032
H4	3.428970380	−0.639031080	−1.568788032

Table 3. Calculated vibrational frequencies of $^{\cdot}CH_2NH_2$.

Wavenumber /cm^{-1}	Intensity /km mol^{-1}	Symmetry	Approximate type of mode
440.50	44.815	A''	H_2C–NH_2 torsion
750.57	313.345	A'	H_2C–NH_2 *cis*-bend
873.70	7.457	A'	H_2C–NH_2 *trans*-bend
1018.50	0.534	A''	H_2C–NH_2 s-twist
1247.28	43.199	A'	C–N str. + sym. bend
1446.08	4.489	A''	H_2C–NH_2 a-twist
1596.86	5.814	A'	CH_2 scissors
1804.77	53.142	A'	NH_2 scissors
3270.03	24.912	A'	CH_2 s-stretch
3379.18	22.363	A''	CH_2 a-stretch
3769.89	9.445	A'	NH_2 s-stretch
3872.09	14.934	A''	NH_2 a-stretch

Excitation energies and oscillator strengths for various Rydberg transitions. Figure 3 shows the UV spectrum of $^{\cdot}CH_2NH_2$ on a wavenumber scale. The low energy part of the spectrum in the range of 27 127–31 000 cm^{-1} is

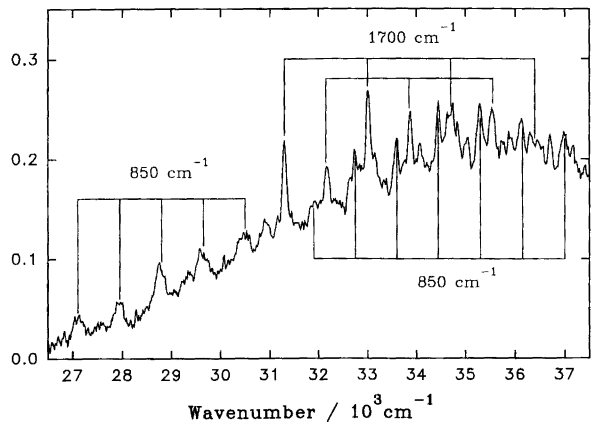

Fig. 3. UV spectrum of CH_2NH_2. Band heads of the Rydberg transitions are located at 27.127 cm^{-1} ($\pi^* \rightarrow 3p_x$) and 31.300 cm^{-1} ($\pi^* \rightarrow 3p_y$). The complex vibrational structure of the $\pi^* \rightarrow 3p_y$ Rydberg transition is presented in Table 5.

Table 4. Electronic transitions from the ground state of $^{\cdot}CH_2NH_2$.

Type of transition	Excitation energy/cm^{-1}	Oscillator strength	Wavelength/nm
$\pi^* \rightarrow 3s$	20 240	38×10^{-5}	494
$\pi^* \rightarrow 3p_x$	27 580	788×10^{-5}	363
$\pi^* \rightarrow 3p_z$	28 150	5×10^{-5}	355
$\pi^* \rightarrow 3p_y$	30 710	1430×10^{-5}	326

composed of a vibronic progression with band shapes that are clearly different from sharp bands occurring at 31.296 cm^{-1} and above. Thus, it appears that at least two different Rydberg transitions are involved, as in the case of the isoelectronic radical $^{\cdot}CH_2OH$.[5,6] A simple analysis based on the Rydberg equation, $E/eV = IP - 13.6/(n-\delta)^2$ may be used to identify the electronic transition.

With $n=3$ and $\delta=1$ for a 3s Rydberg state combined with experimental values of the ionization potentials of 6.10 eV[7] and 7.56 eV[8] for $^{\cdot}CH_2NH_2$ and $^{\cdot}CH_2OH$, we have calculated values of 2.70 eV and 4.16 eV, which may be compared with experimental values of 3.36 eV and 4.34 eV, respectively. Thus, in the case of $^{\cdot}CH_2OH$ the observed band head at 4.34 eV has been assigned to a π–3s Rydberg transition.[6] However, in the case of $^{\cdot}CH_2NH_2$ the observed transition at 3.36 eV does not coincide with the expected Rydberg transition at 2.70 eV. The excitation energies and oscillator strengths obtained by *ab initio* calculations are presented in Table 4. The weak $\pi^* \rightarrow 3s$ transition at 494 nm was not observed in the present investigation, but the wavelength is in agreement with the transition calculated using the Rydberg formula. However, the predicted stronger transitions $\pi^* \rightarrow 3p_x$ and $\pi^* \rightarrow 3p_y$ appear to be in good agreement with the experimental spectrum. The vibronic structure of the $\pi^* \rightarrow 3p_x$ band may be expressed in terms of a main progression, $\nu = 27\,127 + \nu_1 \times 830$ cm^{-1} ($\nu_1 = 0$–4). By comparison with the calculated frequencies in the ground state as shown in Table 3 it appears that a progression with $\Delta\nu = 830$ cm^{-1} may be assigned to an out-of-plane bending mode.

The strong $\pi^* \rightarrow 3p_y$ band starting at 31 300 cm^{-1} shows a complex vibronic structure containing sharp antiresonances.[27] A number of vibronic transitions occur with an average spacing of 850 cm^{-1}. However, the intensity distribution in the range of 31 300–33 000 cm^{-1} indicates that a progression with $\Delta\nu = 1700$ cm^{-1} is more realistic.

As shown in Table 5 the strongest vibronic progression may be expressed by the simple linear equation, $\nu = 31\,300 + \nu_3 \times 1700$ cm^{-1}, beginning at the band head as shown in Fig. 3. A similar progression, $\nu = 32\,150 + \nu_3 \times 1700$ cm^{-1} is displayed by $\nu_2 = 850$ cm^{-1}. The third progression, $\nu = 31\,900 + \nu_2 \times 850$ cm^{-1} with $\nu_2 = 0$–6, is displaced by $\nu_1 = 600$ cm^{-1}. The two progressions with $\Delta\nu = 1700$ cm^{-1} may be assigned to either NH_2-scissors or CH_2-scissors by comparison with the calculated ground state frequencies listed in Table 3. Likewise the progression with $\Delta\nu = 850$ cm^{-1} may be assigned to an H_2C–NH_2 *trans*-bend vibration. A number of weaker lines in the spectrum have not yet been assigned.

Table 5. Vibrational structure of the $\pi^* \rightarrow 3p_y$ Rydberg transition.[a]

Position/cm^{-1}	Vib. energy	Assignment
31 300	0	b(0.0)
31 900	600	$b + \nu_1$
32 150	850	$b + \nu_2$
32 750	1450	$b + \nu_1 + \nu_2$
33 000	1700	$b + \nu_3$
33 600	2300	$b + \nu_1 + 2\nu_2$
33 850	2550	$b + \nu_2 + \nu_3$
34 350	3050	$b + \nu_1 + 3\nu_2$
34 700	3400	$b + 2\nu_3$
35 200	3900	$b + \nu_1 + 4\nu_2$
35 550	4250	$b + \nu_2 + 2\nu_3$
36 050	4750	$b + \nu_1 + 5\nu_2$
36 400	5100	$b + 3\nu_3$
36 900	5600	$b + \nu_1 + 6\nu_2$

[a] $\nu_1 = 600$ cm^{-1}, $\nu_2 = 850$ cm^{-1}, $\nu_3 = 1700$ cm^{-1}.

Conclusions. The UV spectrum of the aminomethyl radical, $^{\cdot}CH_2NH_2$, has been recorded in the range 270–380 nm. Based on the results of *ab initio* calculations we conclude that the spectrum is composed of two Rydberg transitions of which the low energy transition, $\pi^* \rightarrow 3p_x$ starting at 368.6 nm is composed of a fairly strong vibronic progression with an average spacing of $\Delta\nu = 830$ cm^{-1}. The second Rydberg transition, $\pi^* \rightarrow 3p_y$ starting at 319.5 nm shows a complex vibronic structure, which has tentatively been assigned to two displaced progressions with $\Delta\nu = 1700$ cm^{-1} and one with $\Delta\nu = 850$ cm^{-1}. Kinetic studies of the formation and decay of $^{\cdot}CH_2NH_2$ were carried out by monitoring the transient absorption at 319.52 nm. The formation reaction $F^{\cdot} + CH_3NH_2 \rightarrow HF + {}^{\cdot}CH_2NH_2$ was found to proceed with a rate constant of 1.3×10^{-10} cm^3 molecule^{-1} s^{-1}. A lower limit of 8.1×10^{-11} cm^3 molecule^{-1} s^{-1} for the reaction $2\,{}^{\cdot}CH_2NH_2 \rightarrow$ products was derived from the observed second order kinetics based on the assumption that all F-atoms were consumed in the reaction $F^{\cdot} + CH_3NH_2 \rightarrow HF + {}^{\cdot}CH_2NH_2$. In the presence of oxygen the decay rate was found to increase in accordance with the reaction $^{\cdot}CH_2NH_2 + O_2 \rightarrow$ products with a rate constant of $7.8(8) \times 10^{-11}$ cm^3 molecule^{-1} s^{-1}. So far we have not been able to identify the products, O_2–$^{\cdot}CH_2NH_2$ or $HO_2^{\cdot} + N_2C{=}NH$. However, the formation of $H_2C{=}NH$ has been proposed as the major channel in the atmospheric oxidation mechanism of methylamine.[13]

Acknowledgements. Sten Rettrup wishes to acknowledge financial support from The Danish Natural Science Research Council and EEC under the TMR Program.

The authors thank Dr. R. D. Amos for permission to make use of the CADPAC program package.

References

1. Atkinson, R., Perry, R. A. and Pitts, J. N. Jr. *J. Chem. Phys. 66* (1977) 1578.
2. Atkinson, R., Perry, R. A. and Pitts, J. N. Jr. *J. Chem. Phys. 68* (1978) 1850.
3. Masaki, A., Tsunashima, S. and Washida, N. *J. Phys. Chem. 99* (1995) 13126.
4. Pagsberg, P., Nielsen, O. J. and Anastasi, C. In: Clark, R. H. and Hester, R. E., Eds., *Spectroscopy in Environmental Science*, Wiley, Amsterdam 1995, p. 263.
5. Pagsberg, P., Munk, J., Sillesen, A. and Anastasi, C. *Chem. Phys. Lett. 146* (1988) 375.
6. Rettrup, S., Pagsberg, P. and Anastasi, C. *Chem. Phys. Lett. 122* (1988) 45.
7. Burkey, T. J., Castelhano, A. L., Griller, D. and Lossing, F. P. *J. Am. Chem. Soc. 105* (1983) 4701.
8. Dyke, J. M., Ellis, A. R., Jonathan, N., Keddar, N. and Morris, A. *Chem. Phys. Lett. 111* (1984) 207.
9. Benson, S. W. *Thermochemical Kinetics*, Wiley, New York 1976.
10. Holmes, J. L., Lossing, F. P. and Mayer, P. M. *Chem. Phys. Lett. 198* (1992) 211.
11. Rasmussen, O. L., Bjergbakke, E., Lynggaard, B., Pagsberg, P., Kirkegaard, P. CHEMSIMUL, Version 9306, Risø National Laboratory 1993.
12. Masaki, A., Tsunashima, S. and Washida, N. *J. Phys. Chem. 99* (1995) 13126.
13. Schade, G. W. and Crutzen, P. J. *J. Atm. Chem. 22* (1995) 319.
14. Pagsberg, P., Munk, J., Anastasi, C. and Simpson, V. *J. Phys. Chem. 93* (1989) 5162.
15. Pagsberg, P., Ratajczak, E. and Sillesen, A. *Res. Chem. Kinet. 1* (1993) 65.
16. Duxbury, G. and Le Lerre, M. L. *J. Mol. Spectrosc. 92* (1982) 326.
17. MOLPRO is a package of *ab initio* programs written by H.-J. Werner and P. J. Knowles, with contributions from J. Almlöf, R. D. Amos, A. Bering, M. J. O. Deegan, F. Eckert, S. T. Elbert, C. Hampel, R. Lind, W. Meyer, A. Nicklass, K. Peterson, R. Pitser, A. J. Stone, P. R. Taylor, M. E. Mura, P. Pulay, M. Schuetz, H. Stoll, T. Thorsteinsson and D. L. Cooper.
18. Dunning, T. H. Jr. *J. Chem. Phys. 53* (1970) 2823.
19. Roothaan, C. C. J. *Rev. Mod. Phys. 32* (1960) 179.
20. Dyke, J. M., Lee, E. P. F. and Zamanpour Niravan, M. H. *Int. J. Mass. Spectrom. Ion. Proc. 94* (1989) 221.
21. Knowles, J. P. and Werner, H.-J. *Chem. Phys. Lett. 145* (1988) 514.
22. Werner, H.-J. and Knowles, J. P. *J. Chem. Phys. 89* (1988) 5803.
23. Knowles, J. P. and Werner, H.-J. *Chem. Phys. Lett. 115* (1985) 259.
24. Knowles, J. P. and Werner, H.-J. *Theor. Chim. Acta 84* (1992) 95.
25. Werner, H.-J. and Knowles, J. P. *J. Chem. Phys. 82* (1985) 5053.
26. CADPAC, The Cambridge Analytical-Derivative Package Issue 5, Cambridge 1992, written by R. D. Amos with contributions from I. L. Alberts, J. S. Andrews, S. M. Colwell, N. C. Handy, D. Jayatilka, P. J. Knowles, R. Kobayashi, N. Koga, K. E. Laidig, P. E. Malsen, C. W. Murray, J. E. Rice, J. Sanz, E. D. Simandiras, A. J. Stone and M. D. Su.
27. Jortner, J. and Morris, G. C. *J. Chem. Phys. 51* (1969) 3689.

Received March 19, 1999.